Transactions, SMiRT-22
San Francisco, California, USA - August 18-23, 2013
Division IX (include assigned division number from I to X)

COMPRESSIVE CHARACTERISTICS OF STEEL PLATE-CONCRETE STRUCTURES USING ECO-ORIENTED CEMENT CONCRETE

Cheol-Kyu Kang[1], Daniel J. Choi[2], Ho-Young Park[3], and Byong Choi[4]

[1]Research Assistant Professor, Ph.D., Dept. of Plant Architectural Engineering, Kyonggi University, S. Korea
[2]Junior Student, Newport High School, Bellevue, WA 98006
[3] Graduate Student, Dept. of Plant Architectural Engineering , Kyonggi University, S. Korea
[4] Professor, Ph.D., P.E., Dept. of Plant Architectural Engineering, Kyonggi University, S. Korea (bjchoi@kgu.ac.kr)

ABSTRACT

The main objective of this study is to describe the compression of steel plate-concrete (SC) walls using eco-oriented cement concrete behavior, and to determine the squash load. The major parameters in this research are the material of the concrete and width-thickness (B/t) ratio of the surface steel plate. Six SC wall specimens were tested in compression in this experiment. In the three specimens, necessary to reduce emissions of carbon dioxide (CO_2), some of the cement (in weight) was replaced by the Hwangtho (red clay); this clay is a traditional and an environmental material. The maximum compressive strength, specifically the buckling behavior of the surface steel plate and the effective buckling length factors, are discussed based on the test results.

INTRODUCTION

Steel plate-concrete (SC) structures are composed of a steel plate, concrete and shear connectors that combine two materials that are inhomogeneous. They have better structural performance than that of bare steel, or reinforced concrete structures. The research of SC structures have been focused on the use of high strength steel and concrete, that are applied to the special structures such as a nuclear power plant and high-rise buildings. There are many advantages in SC structures, such as the possibility of prefabricated production and modular construction. These advantages provide to excellent potential for the use of the SC structures in mid to low-rise general buildings. A number of researchers are actively studying SC structures , Choi et al.(2009), Dababo et al.(2009), Han et al.(2008), Kanchi et al.(1996), Kwon et al.(2011), Liu et al.(2003 and 2005), McKinley et al.(2002), Takeuchi et al.(1998), Tao et al.(2008 and 2009), Vercelj et al.(2002) and Uy et al.(2001 and 2011). However, the number of past test specimens subjected to compressive loading, is limited because they have used the ordinary or high strength concrete in SC structures. This research tried to establish some basic design information of SC structures toward mid to low-rise general buildings using eco-oriented cement concrete. For this reason some of the experimental specimens used Hwangtho (red clay), instead of cement in the concrete mixture. In this research, these specimens are called eco-oriented cement concrete. The objective of this study is threefold : (1) To experimentally investigate the behavior of SC walls with normal and eco-oriented cement concrete subjected to axial loading; (2) To compare the test results with those predicted, using KEPIC-SNG(2010) and JEAG-4618(2005); (3) To evaluate the effective buckling length factors for surface steel plate buckling.

BRIEF REVIEW OF CODE-SPECIFIED DESIGN STRENGTHS FOR SC STRUCTURES

A brief review of how the compressive strength of SC structures is determined, is provided as follows:

The KEPIC-SNG(2010)

The nominal compression on strength for axially-loaded SC wall structures shall be determined for the limit state of flexural buckling including local buckling of the steel plate as follows

(1) $P_e \geq 0.44\,P_o$;

$$P_n = \left[0.658^{\frac{p_o}{P_e}} \right] p_o \tag{1}$$

(2) $P_e < 0.44\,P_o$;

$$P_e < 0.44 P_o \tag{2}$$

Where,

$$P_o = 2A_p F_{cr} + 0.85 A_c f_{ck} \tag{3}$$

$$P_e = \frac{\pi^2 E I_{eff}}{(K_w L)^2} \tag{4}$$

$$F_{cr} = (1.5 - 0.043\frac{K_p B}{t_p} - 90\varepsilon_n) F_{yp} < F_{yp} \tag{5}$$

The JEAG-4618(2005)

Researchers in Japan performed a series of compression tests using SC wall structures, and evaluated the squash load. Based on this research, AIJ suggested Eq. (6) to estimate the compressive strength of the SC wall structures, as follows.

$$P_{JEAG} = F_{cr} A_s + f_{ck} A_c \tag{6}$$

(1) $B/t \leq 600/\sqrt{F_y}$;

$$F_{cr} = F_y \tag{7}$$

(2) $B/t > 600/\sqrt{F_y}$;

$$F_{cr} = F_e \tag{8}$$

Where,

$$F_e = \frac{\pi^2 E_s}{12K^2 (B/t)^2} \tag{9}$$

TEST PROGRAMS

Test Specimens

The test specimens were classified into two groups, elastic and inelastic buckling specimens. The stud ratio (B/t) to classify the elastic and inelastic buckling was derived as Eq. (11) from Eq. (10).

$$\varepsilon_{cr} = \frac{\pi^2}{12K^2 (B/t)^2} = \frac{\sigma_y}{E_s} \tag{10}$$

Where E_s is 205,000 MPa and k is assumed 0.7.

$$B/t = 600/\sqrt{F_y} \tag{11}$$

The average tensile yield strength of steel plate was 428 MPa from the test. Therefore, the specimens were set elastic and inelastic buckling on the basis of B/t=29. The B/t=20 specimens were expected to buckled in the inelastic range whereas the B/t=30 and B/t=40 specimens were expected to buckled in the elastic range. A total of 6 specimens, including 3 ordinary cement concrete specimens and 3 eco-oriented cement concrete specimens, subjected to axial compression were tested.

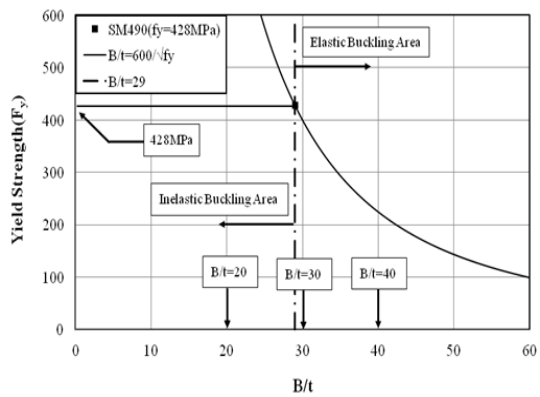

Figure 1. Elastic and inelastic buckling range

Table 1: List of specimens

No	Specimen	Material	B/t	f_{ck} (MPa)	Specimen Size(mm)		
					thickness	width	Height
1	C24/490-T6B20	Cement	20	24	250	280	380
2	C24/490-T6B30	Cement	30	24	250	370	500
3	C24/490-T6B40	Cement	40	24	250	460	620
4	H16/490-T6B20	Cement+Hwangtho	20	16	250	280	380
5	H16/490-T6B30	Cement+Hwangtho	30	16	250	370	500
6	H16/490-T6B40	Cement+Hwangtho	40	16	250	460	620

C : Cement
H : Eco-oriented Cement (Hwangtho+cement)
24 : Compressive strength of Concrete (16=16MPa,24=24MPa)
490 : Yield strength of surface steel plate (490 = SM490)
T6 : Surface steel plate thickness (6 mm)
B20 : Width-thickness ratio(B/t = 20, 30, 40)

The main parameters varied in the tests were as follows.

- Material of the concrete : normal cement, eco-oriented cement (Cement+Hwangtho)
- Thickness of the steel plate : 6mm
- Stud ratio (B/t) : 20, 30, 40

A summary of the specimens is presented in Table 1, where the diameter of the stud connector was 13mm and the length was 108mm.

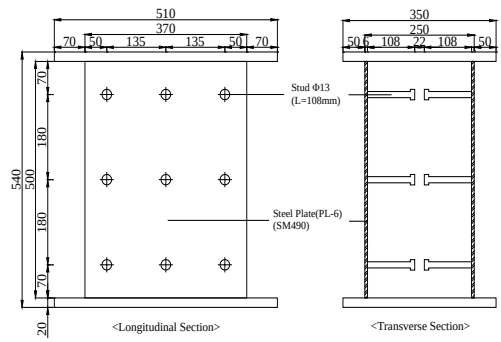

Figure 2. Test specimen

Material Properties

Three coupons were prepared from the steel sheet according to the requirements in KS B 0801 and were tested at a loading rate of 0.5 mm/min before the yield load, and 1mm/min after the yield load. The average yield stress, tensile strength and modulus of elasticity were determined as 428, 534 and 202,000MPa, respectively. The tensile test results are identified in Table 2.

Table 2: Results of tensile test

Steel plate	thickness (mm)	Yield strength (MPa)	Tensile strength (MPa)	Elastic Modulus (MPa)	Yield Ratio (%)	Ductility (%)
SM490	6.0	428	534	2.02E5	80	36

Concrete was mixed in two batches. From each batch, three cylinders (diameter of 150 mm and height of 300 mm) were prepared. The concrete samples were cured in the molds covered by wet clothes to simulate the actual curing condition of the concrete inside the steel plate. The two end surfaces of the concrete cylinders were ground flat before compressive tests. Table 3 summarizes the details of the mix proportions and measured material properties of the two batches of concrete.

Table 3: Details of the mix proportions and measured material properties

Batch No.	Cement (N/m^3)	Water (N/m^3)	Hwangtho (N/m^3)	Sand (N/m^3)	Coarse aggregate (N/m^3)	Average cylinder strength (MPa)
OPC	3,626	1,813	0	7,428	10,123	24
H20	2,900	1,813	725	7,134	10,084	16

Test Procedure

A 5,000kN capacity testing machine was used for the compression tests of all specimens, as shown in Figure 3(a). The preliminary tests within the elastic range were conducted by carefully adjusting the position of the specimen to ensure uniform compression, based on the measurements of four displacement transducers attached at the mid-height of the test specimen.

Four linear voltage displacement transducers (LVDTs) were used to measure the axial shortening during the tests, as shown in Figure 3(b). Several strain gauges were used for each specimen to measure the strains of the plate at different positions (Figure 3(c).). In addition, two strain gauges were bonded at the top and bottom of each stud to identify the tensile behavior of the studs, as shown in Figure 3(c).

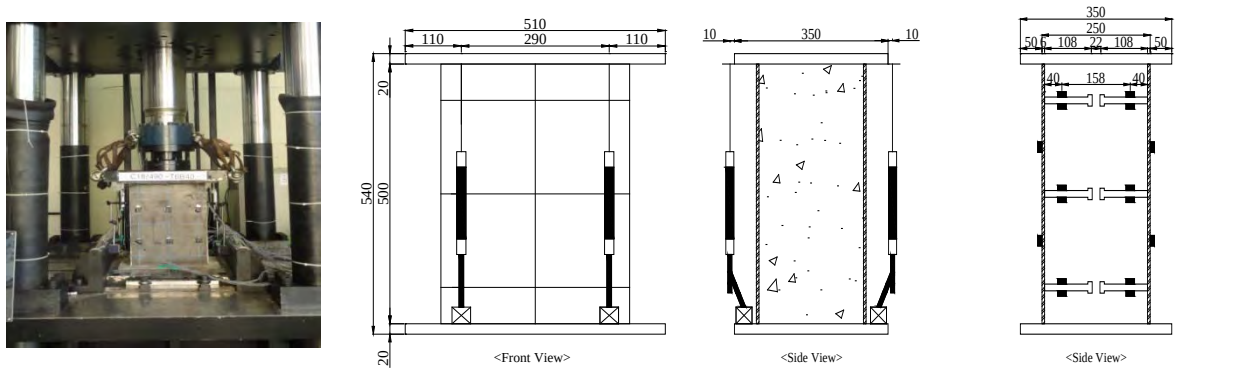

(a) Test set-up (b) Installation of LVDT (c) Installation of strain gauge

Figure 3. Test set-up of specimens

The specimens were loaded continuously until they failed. All specimens were tested under displacement control so that the full displacement to failure, and the resultant ductility could be observed. A load interval of less than one-tenth of the estimated load carrying capacity was used. Each load interval was maintained for about 2-3 minutes.

ANALYSIS OF TEST RESULTS AND DISCUSSION

Maximum Compressive Loads

This section presents information on the maximum compressive strength of the test specimens. Table 4 provides comparisons of the measured values of compressive strength with the predicted compressive strength presented in section 2.

Table 4: Comparison of compressive strength (kN)

No. (1)	Specimen (2)	Test Value (3)	Eq. (3) (4)	Eq. (6) (5)	Ratio(%)	
					(3)/(4)	(3)/(5)
1	C24/490-T6B20	3052	2639	3037	115.6	100.5
2	C24/490-T6B30	3528	3079	3811	114.6	92.6
3	C24/490-T6B40	4164	3320	3814	125.4	109.2
4	H16/490-T6B20	2539	2186	2504	116.1	101.4
5	H16/490-T6B30	3055	2480	3106	123.2	98.3
6	H16/490-T6B40	3812	2575	2938	148.0	129.7
No.1~No.3 average		-	-	-	118.5	100.8
No.4~No.6 average		-	-	-	129.1	109.8
Total average		-	-	-	123.8	105.3
Standard deviation		-	-	-	11.5	11.9

Column (3) of this table lists the compressive strength values measured in the tests. Column (4) lists the strength predicted using Eq. (3), KEPIC-SNG and column (5) lists the strength predicted by Eq. (6), JEAG-4618

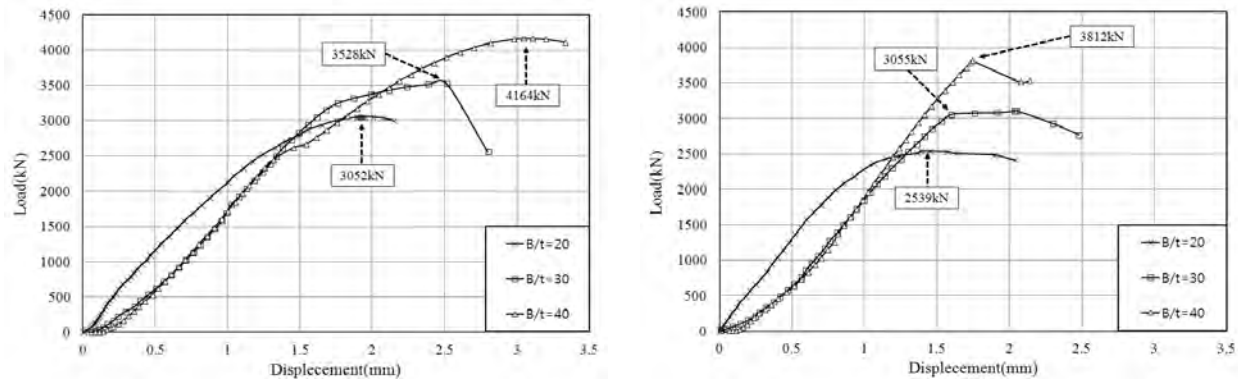

(a) Ordinary Portland cement concrete (b) Eco-oriented cement concrete

Figure 4. Load-displacement relationship

The maximum compressive strengths increased with an increase of the B/t ratio from 20 to 40 due to the difference of the specimen size, as shown in Table 4 and Figure 4. It was proven that the safety margin for the estimation of compressive strength, using ordinary cement (No. 1~ No. 3 specimens) was about 18.5 % and 0.8%, based on Eq. (3) and (6) respectively. For the estimation of compressive strength using eco-oriented cement (No. 4~ No. 6 specimens), however, the safety margin showed about 29.1 % and 9.8 %, based on Eq. (3) and (6), respectively.

Analysis Of Plate Buckling Using Column Theory

The buckling load of the surface plate was calculated from a column theory regarding the plate with the column between each stud, as shown in Figure 5.

The Euler buckling load for these columns subjected to axial compression, can be expressed as follows.

$$P_{cr} = \frac{\pi^2 EI}{(kl)^2} \tag{12}$$

The elastic buckling strain can be determined from Eq. (12).

$$\varepsilon_{cr,Euler} = \frac{\pi^2}{12k^2(B/t)^2} \tag{13}$$

The slenderness parameter λ_c, which is adopted in AISC-LRFD, was derived to apply the SC structures.

(1) $\lambda_c \le 1.5$

$$\varepsilon_{cr,LRFD} = (0.658^{\lambda_c^2})\varepsilon_y \tag{14}$$

(2) $\lambda_c > 1.5$

$$\varepsilon_{cr,LRFD} = \left(\frac{0.877}{\lambda_c^2}\right)\varepsilon_y \tag{15}$$

$$\lambda_c = \frac{\sqrt{12}\cdot K}{\pi}\cdot\frac{B}{t}\sqrt{\frac{F_y}{E}} \tag{16}$$

Figure 6. shows the strain versus B/t ratio curves using equations from (13) to (16) when the effective length factor was 0.5 and 0.7. In Figure 6, the symbols designated the measured value from the location of where the buckling occurred in the specimens.

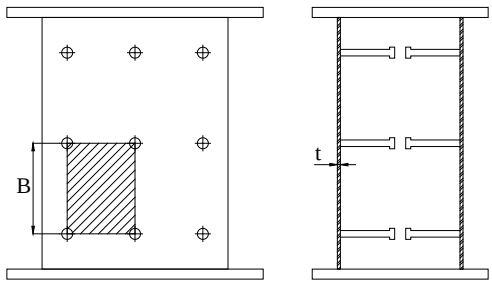

Figure 5. B/t ratio to apply the column theory

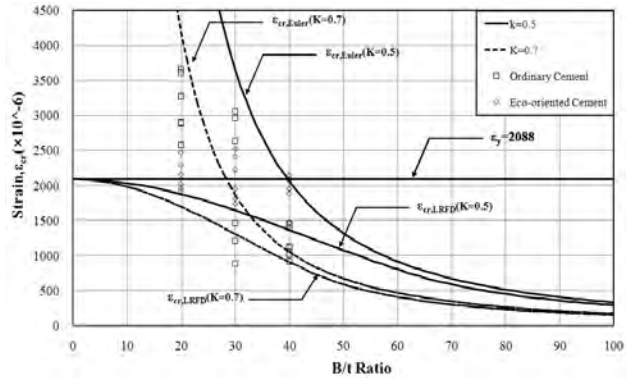

Figure 6. B/t ratio vs. strain of surface steel plate

For specimens with B/t=20, ranging inelastic buckling, the measured strains did not exceed the Euler's elastic curve (Eq. 13), regardless of specimens using the ordinary or eco-oriented cement concrete. However, the measured strains exceeded the AISC-LRFD curve (Eq. 14 and 15) for all specimens.

For specimens with B/t=30, ranging elastic buckling, the measured strains exceeded the Euler's elastic curve when the effective length factor was 0.7. However, the measured strains did not reach the Euler's elastic curve when the effective length factor was 0.5, regardless of whether the specimens used the ordinary or eco-oriented cement concrete. The measured strains for all specimens exceeded the AISC-LRFD curve when the effective length factor was 0.7 and 0.5.

For specimens with B/t=40, the measured strains for specimens using the ordinary cement concrete exceeded the Euler's elastic curve when the effective length factor was 0.7; however, the measured strains did not reach the curve when the effective length factor was 0.5. The measured strains for that specimen exceeded the AISC-LRFD curve when the effective length factor was 0.7 and 0.5. For specimens using the eco-oriented cement concrete, the measured strains exceeded the Euler's elastic and AISC-LRFD curves when the effective length factor was 0.7 and 0.5.

For the plate buckling that used the column theory, the more B/t ratio approaches the elastic range, the more measured strains exceeded the Euler's elastic curve. For the elastic buckling range, the behavior of specimens with the eco-oriented cement concrete was more stable than that of specimens with the ordinary cement concrete. It can be found that the effective length factor of the specimen with eco-oriented cement concrete, the effective length factor of 0.5 could be applied in the AISC-LRFD curve.

The effective length factor was derived from eq. (13) as follows.

$$k = \sqrt{\frac{\pi^2}{12\varepsilon(B/t)^2}} \tag{17}$$

In Eq. (17), strains of the plate used the measured value from the specimens. The effective length factors calculated from eq. (17) versus B/t ratio of the specimens are shown in Figure 7. The values of effective length factor for specimens with ordinary cement concrete were varied between 0.58 to 0.75, and an average was calculated as 0.65. For specimens with eco-oriented cement concrete, the values of those varied from 0.47 to 0.59, and the average was calculated as 0.51.

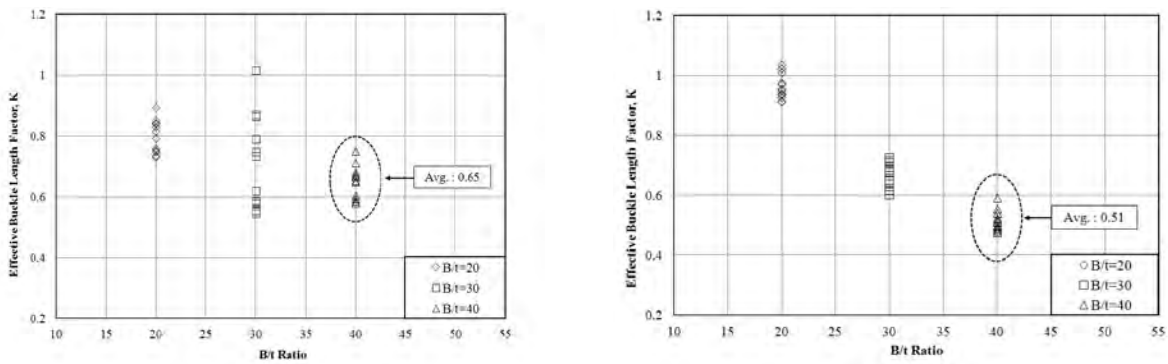

(a) Ordinary Portland cement concrete (b) Eco-oriented cement concrete

Figure 7. Effective length factor, k

Analysis Of Plate Buckling Using Plate Theory

The buckling load of the surface plate was calculated from the plate theory regarding the plate as a unit plate between each stud, as shown in Figure 8(a).

The elastic buckling stress by the plate theory is as follows.

$$\sigma_{cr,pl} = k_{pl} \frac{\pi^2 E}{12(1-v)^2 (\overline{B}/t)^2} \tag{18}$$

The effective length factor of plate is expressed as follows.

$$k_{pl} = \left(\frac{m}{\alpha}\right)^2 + 2n^2 + n^4 \left(\frac{\alpha}{m}\right)^2 \tag{19}$$

The value of n in Eq. (19) must be unit value to obtain the critical buckling stress. Therefore, the effective length factor can be simplified as follows.

$$k_{pl} = \left(\frac{m}{\alpha} + \frac{\alpha}{m}\right)^2 \tag{20}$$

The effective length factors were calculated as 7.63 for specimens with B/t=20, 6.46 for specimens with B/t=30 and 5.95 for specimens with B/t=40, respectively. By substitute, B with($\overline{B}$), specimens with B/t=20 correspond to $\overline{B}$/t=47, specimens with B/t=30 correspond to $\overline{B}$/t=62 and specimens with B/t=40 correspond to $\overline{B}$/t=77, respectively. Figure8 showed the $\overline{B}$/t ratio versus strains of the surface steel plate where the symbols designated the measured value from the location of buckling occurred in the specimens.

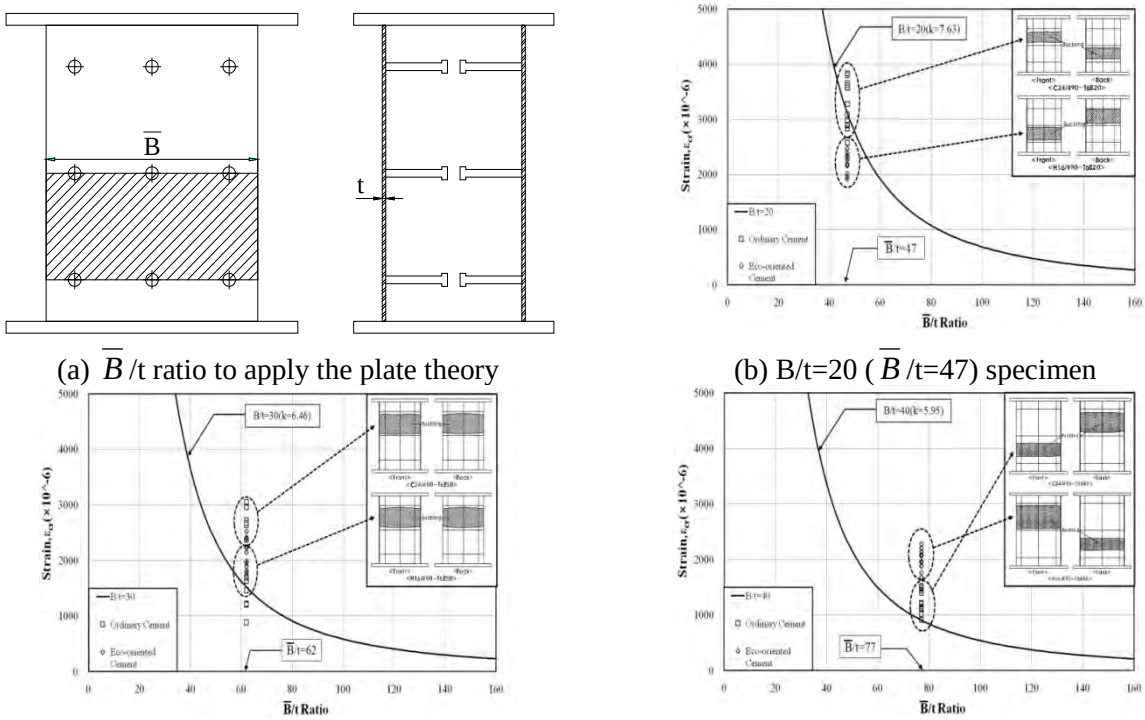

(a) $\overline{B}$/t ratio to apply the plate theory (b) B/t=20 ($\overline{B}$/t=47) specimen

(c) B/t=30 ($\overline{B}$/t=62) specimen (d) B/t=40 ($\overline{B}$/t=77) specimen

Figure 8. $\overline{B}$/t ratio vs. strain of surface steel plate using plate theory

For specimens with B/t=20, ranging inelastic buckling, the measured strains approached or exceeded the elastic buckling strains (Eq. 18) for the specimens using the ordinary cement concrete. The measured strains, however, did not reach the elastic buckling strains for the specimens using the eco-oriented cement concrete.

For specimens with B/t=30 and B/t=40, the measured strains resulted in values that were somewhat higher than that of the plot by elastic buckling strains (Eq. 18).

CONCLUSION

In this study, the overall results of the compression test were presented, with the focus on the material properties of the concrete. The maximum compressive strength, the effective length factor and the buckling behavior of the surface steel plate were investigated. Based on the results of the test and the investigation, the following conclusions were drawn:

For the specimens using ordinary cement concrete, the compressive strength resulted in an experiment range from 115% to 125% of the nominal strength calculated from the design equation of the KEPIC-SNG. The safety margin for the estimation of compressive strength was about 19%, based on the design equation of the KEPIC-SNG. The compressive strength resulted in an experiment range from 116% to 148% of the nominal strength calculated from the design equation of the KEPIC-SNG for the specimens using eco-oriented cement concrete. The safety margin for the estimation of compressive strength was about 29%, based on the design equation of the KEPIC-SNG.The effective buckling length factor when applied to the column theory was about 0.65 for the specimens using ordinary cement concrete. For the specimens using eco-oriented cement concrete, this factor was about 0.51.

ACKNOWLEDGEMENTS

The authors would like to express their deep appreciation for the generous support given by the National Research Foundation of Korea (No.2011-0026221).

NOTATIONS

A_c	: area of the concrete.	A_p	:area of the steel plate on one side.
A_s	: area of the surface steel plate.	B	: distance between headed studs.
Bt	: area of a steel plate between the studs	E_s	: the elastic modulus of a steel plate
F_{ck}	: specified compressive strength of concrete.	F_{cr}	: local buckling stress of the surface steel plate.
F_{yp}	: yield strength of the surface steel plate.	k	: coefficient of effective length factor in Euler column theory
k_{pl}	:coefficient of effective length factor in plate buckling theory	t	: thickness of the surface steel plate
ε_{cr}	: measured buckling strain of a steel plate	ε_n	: nominal compressive strain

REFERENCES

AIJ, JEAG 4618. (2005), Technical guidelines for seismic design of steel plate concrete structures: for buildings and structures.

Choi, B. J. et al, (2009), “An experiment on compressive profile of the unstiffened steel plate-concrete structures under compression loading”, Steel and composite structures An International Journal, Vol. 9, No 6, 519-534.

Dababo M. A. et al, (2009), “Experimental investigation on concrete-filled stainless steel stiffened tubular stub columns”, Engineering Structures, Vol. 31, 300-307.

Dabaon M. et al, (2009), “confinement effect of stiffened and un-stiffened concrete-filled stainless steel tubular stub columns”, Journal of construction Steel Research, Vol. 65, 1846-1854.

Galambos, Theodore V. (1998), Guide to stability criteria for metal structures, 5th ed., John Wiley & Sons Inc.

Han, L.H. et al, (2008), “Behavior of thin walled steel tube confined concrete stub columns subjected to axial local compression”, Thin-Walled Structures, Vol. 46, pp. 155-164

Kanchi, Maski et al. (1996), “Experimental study on a concrete-filled steel structure, compressive test (1),”Architectural Institute of Japan Conference Part 2, pp. 1071-1072.

Kim, W. B. and Choi, B. J. (2011), “Shear strength of connections between open and closed steel-concrete composite sandwich structures”, Steel and composite structures An International Journal, Vol. 11, No 6, 169-181.

Korea Electric Association (KEA). (2010), Steel-concrete structures (KEPIC-SNG), Korea Electric Power Industry code.

Kwon, Y. B. et al (2011), “Prediction of the squash loads of concrete-filled tubular section columns with local buckling”, Thin-walled Structures, Vol. 49, 85-93.

Liang, Q.Q, Uy, B. and Richard Liew J.Y. (2006), “Nonlinear modeling and evaluation of concrete-filled steel tubular columns with local buckling effects,” Journal of Construction Steel Research, 62(6), pp. 581-591

Liu, D. et al. (2003), “Ultimate capacity of high-strength rectangular concrete-filled steel hollow section stub columns,” Journal of Construction Steel Research , 59, pp.1499-1515

Liu, D. (2005), “Tests on high-strength rectangular concrete-filled steel hollow section stub columns,” Journal of Construction Steel Research, 61, pp. 902-911

LRFD , AISC. (2005), Load and Resistance Factor Design Specification, 2005

McKinley, B., and Boswell, L.F. (2002), “Behavior of Double skin composite construction,” Journal of Construction Steel Research, Vol 58.

Miyauchi, Yasuyoshi et al. (1996), “Experimental study on a concrete-filled steel structure, compressive test (2),”Architectural Institute of Japan Conference, Part 2, pp. 1073-1074.

Takeuchi, M. et al. (1998), “Study on a concrete-filled structure for nuclearpower plants”, Nuclear

Engineering and Design 198, 1998, pp. 209-223.

Tao, Z. el al. (2008), "Strength and ductility of stiffened thin-walled hollow steel structural stub columns filled with concrete," Thin-Wall. Structure, 46(10), pp.1113-1128

Tao, Z. el al. (2009), "Analysis and design of concrete-filled stiffened thin-walled steel tubular columns under axial compression," Thin-Wall. Structure, 47, pp.1544-1556

Uy, B. (2001), "Strength of short concrete filled high strength steel box columns," Journal of Construction Steel Research, 57(2), pp.113-134

Uy, B. et al, (2011), "Behavior of short and slender concrete-filled stainless steel tubular columns," Journal of Construction Steel Research, 67(2), pp.360-378

Vrcelj, Z. and Uy. B. (2002), "Strength of slender concrete-filled steel box columns incorporating local buckling," Journal of Construction Steel Research, 58(2), pp. 275-300